

# DETECTION OF RADIOACTIVE MATERIAL ENTERING NATIONAL PORTS: A BAYESIAN APPROACH TO RADIATION PORTAL DATA<sup>1</sup>

BY SIDDHARTHA R. DALAL AND BING HAN

*RAND Corporation*

Given the potential for illicit nuclear material being used for terrorism, most ports now inspect a large number of goods entering national borders for radioactive cargo. The U.S. Department of Homeland Security is moving toward one hundred percent inspection of all containers entering the U.S. at various ports of entry for nuclear material. We propose a Bayesian classification approach for the real-time data collected by the inline Polyvinyl Toluene radiation portal monitors. We study the computational and asymptotic properties of the proposed method and demonstrate its efficacy in simulations. Given data available to the authorities, it should be feasible to implement this approach in practice.

**1. Introduction.** With increased terrorism around the world and instability in some nuclear-capable nations, there is a growing national safety concern about terrorists bringing illicit nuclear materials into the U.S. Substantial efforts have gone into devising strategies for inspecting containers and intercepting various types of illicit nuclear material. In the U.S. there are 307 ports of entry representing 621 official air, sea and land border crossing sites, through which approximately 57,000 containers enter the borders every day. For effective inspection without increasing traffic congestion, the U.S. Department of Homeland Security has adopted a multilayered approach to inspection, which consists of an analysis of customs documents, followed by an inline automatic inspection of the containers, and an offline stringent manual inspection for suspicious containers. For more details of the process and the corresponding risk analysis, we refer to [Wein et al. \(2006\)](#) and [Martonosi, Ortiz and Willis \(2006\)](#).

One objective of the inline preliminary inspection procedure is to identify radioactive cargo that is being shipped in a container. The inline preliminary inspection procedure consists of scanning containers in a radiation portal monitor (RPM) via a gamma ray Polyvinyl Toluene (PVT) scanner. Currently, 98% of incoming containers go through this radiation scanning situated at most ports of entry. Based on the data collected during scanning, the inline inspection procedure makes a quick automatic decision to let a container pass or to scrutinize it further with the

---

Received August 2009; revised January 2010.

<sup>1</sup>Supported in part by NSF Grant CBET-0736134.

*Key words and phrases.* Bayesian classifier, Poisson model, nuclear detection, terrorism, machine learning.

offline process. In addition, a few containers are randomly selected for offline inspection. For example, the Los Angeles Times (11/26/2004) reported that at the Los Angeles port in 2004, around 12,000 containers arrived daily and, on average, 43 were inspected by hand.

The design of the RPM consists of a drive-through portal with passive PVT sensors that detect gamma rays emitting from a source. At an inspection point, the container is driven through the portal at low speed (4–5 mph), taking around 20 seconds. The portal captures the radiation counts at every 0.1-second interval in a number of energy channels ranging from low to high. For example, the portals manufactured by SAIC in certain configurations have 256 channels. The next generation of portals based on Sodium Iodide Scintillators will have 1024 channels. The collected data consist of the radiation count in each of the channels at every 0.1-second interval, accumulated over 1 second. In practice, the data are further aggregated over multiple channels in a number of nonoverlapping coarser windows. Typical configurations involve 2–8 nonoverlapping exhaustive windows from very low energy to very high energy. In our paper we focus on nonoverlapping energy windows, referred to as windows in the rest of this paper. For an excellent exposition of the details related to energy windowing, we refer to [Ely et al. \(2004\)](#) and [Ely et al. \(2006\)](#).

Given that the distance from the source changes as a container is driven through the portal, radiation counts will also change. The upper frame of [Figure 1](#) shows an example of radiation count data as a container is rolling through a radiation portal (courtesy of Pacific Northwest National Laboratory). The figure depicts readings of a container passing through a 2-window system corresponding to the high- and low- energy windows. The upper frame of the figure superposes the readings of the two windows with the different scales on the left- and right-hand axes, while the lower frame plots the ratio of low- to high-energy readings. Currently, only the total count corresponding to the distance which yields the maximal total count is used for detection purposes. When the total count exceeds a preset threshold, a container is classified as potentially dangerous. However, this crude method may fail to detect dangerous man-made sources in small quantities when mixed with naturally occurring radioactive materials. In [Section 5](#) we show a numerical example where all containers have approximately the same mean total count, which the current inspection cannot differentiate.

In this paper we propose a decision theoretic approach based on Bayesian methods for identifying suspicious containers using the data collected during the inline inspection. This paper is organized as follows. In [Section 2](#) we introduce the available RPM data collected by the inline inspection system, and describe a statistical model for the RPM data based on a Poisson process. In [Section 3](#) we introduce the machinery needed for a Bayesian approach and propose a naive Bayesian classifier. In [Section 4](#) we show that the proposed procedure is asymptotically accurate in the sense that the probability of misclassification goes to zero as the mean radiation counts become large. In [Section 5](#) we explore the efficacy of our procedure

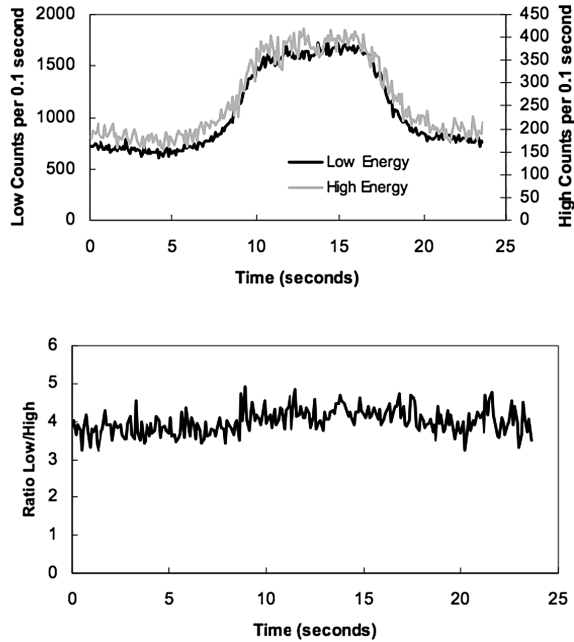


FIG. 1. Gamma counts as a container of NORM passes a 2-window PVT. The container passes through the portal for around 23 seconds. The upper frame shows the superposition of the low- and high-energy windows with different scales. The lower frame gives the ratio of counts between the two windows.

by numerical examples based on real energy spectra for exact classification. We also propose an algorithm to simplify the classifier when the objective is limited to discriminating between dangerous and nondangerous materials. Finally, this paper concludes with a discussion of some of the implementation challenges and future extensions.

**2. The Poisson model for radiation emission data.** A container may include man-made radioactive material of high concern, including Highly Enriched Uranium (HEU) or Weapons Grade Plutonium (WGPu), as well as other common classes of cargo that have been officially declared in filings with Customs. Some common classes are naturally occurring radioactive materials (NORM) and are often misclassified based on the currently deployed methodologies during inline inspection. Some common NORM classes include fertilizer, kitty litter and refractory material. The radioactivity in NORM is caused by some ingredients with natural radioactivity, for instance, clay from some regions in Mexico.

For the remainder of this paper, we tackle the objective of classifying a container into one of  $K$  classes. Initially we consider each class to be either a NORM or a man-made nuclear material. Later on we shall discuss the situation involving mixtures of materials. We first introduce the notation for the radiation data.

Let  $Y$  denote the class variable,  $Y = k$  if the container being inspected is in the  $k$ th class. Let  $\mathbf{Z}$  denote all of the radiation count data obtained at a RPM with  $B$  windows corresponding to a particular container. Let  $\mathbf{R}_d = (R_{1,d}, \dots, R_{B,d})'$  denote the vector of counts at a distance  $d = d(t)$  away from the detectors. Time  $t$  is used as the surrogate of  $d$  in Figure 1.  $\mathbf{Z}$  is a  $B \times T$  matrix

$$(1) \quad \mathbf{Z} = (\mathbf{R}_{d(1)}, \mathbf{R}_{d(2)}, \dots, \mathbf{R}_{d(T)}) = \begin{pmatrix} R_{1,d(1)} & R_{1,d(2)} & \dots & R_{1,d(T)} \\ R_{2,d(1)} & R_{1,d(2)} & \dots & R_{2,d(T)} \\ \dots & \dots & \dots & \dots \\ R_{B,d(1)} & R_{B,d(2)} & \dots & R_{B,d(T)} \end{pmatrix},$$

where  $T$  is the total number of sampling times,  $t = 1, \dots, T$ . Finally, let  $N_d$  denote the total counts at distance  $d$ ,  $N_d = \sum_b R_{b,d} = \mathbf{1}'\mathbf{R}_d$ .

Poisson models have been frequently used in modeling radiation counts and other types of emission counts [Karlin and Taylor, 1998]. We use the following Poisson process model (2) for the RPM count data, which will be subsequently used to build a naive Bayesian classifier in the next section. Let  $M$  be the quantity of material in a container, and let  $\lambda_{b,k}$  be the emission rate for a unit quantity of class  $k$  in window  $b$  at the distance  $d = 0$ . Given that a container has  $M$  quantity of the  $k$ th material class and is at distance  $d$  from the detector,

$$(2) \quad R_{b,d} | (Y = k, d, M) \sim \text{Poisson}(g(d, M)\lambda_{b,k})$$

$$b = 1, \dots, B, d = d(1), \dots, d(T),$$

where all  $R_{b,d}$  are independent, and  $g(d, M)$  is an unknown function. One would expect  $g(d, M)$  to be decreasing in distance  $d$  and increasing in quantity  $M$ , with  $g(0, 1) = 1$ . The specific form of  $g$  depends on the physical mechanism of sensors, signal processing and various environmental factors.

Ely et al. (2004) and Ely et al. (2006) delve into a substantive discussion of  $g(d, M)$  through the amount of information available in  $N_d$ , which they find is very unreliable. Moreover, the function  $g$  is associated not only with distance  $d$  and amount of material  $M$ , but also with various environmental conditions (e.g., weather and background noise), vehicle shielding (which varies from container to container), and a container’s angular placement relative to the detectors (which changes as the vehicle traverses through the portal), and sensitivity of sensors. Thus,  $g$  is a function of many more variables than just the quantity and distance. Modeling  $g$  would be very difficult since many factors are unknown or not collected. We will not pursue this parametric line of inquiry here because of the inherent difficulties mentioned above and the lack of publicly available data.

Given the difficulties in modeling  $g$ , we consider  $g$  as a nuisance parameter and remove it for inference by appropriate conditioning. To realize this, note that  $N_d$  follows independent Poisson distributions with mean  $g(d, M) \sum_b \lambda_{b,k}$ . By construction, the conditional distribution is

$$P(\mathbf{R}_d | N_d, Y = k, d, M) \propto P(R_{1,d}, \dots, R_{B,d}, N_d | Y = k, d, M)$$

$$= P(R_{1,d}, \dots, R_{B,d} | Y = k, d, M).$$

We then have

$$\begin{aligned}
 &P(R_{1,d}, \dots, R_{B,d} | Y = k, d, M, N_d) \\
 (3) \quad &\propto \prod_b [g(d, M)\lambda_{b,k}]^{R_{b,d}} / (R_{b,d}!) \\
 &\propto \frac{N_d!}{R_{1,d}! \cdots R_{B,d}!} \left( \frac{\lambda_{b,k}}{\lambda_k} \right)^{R_{b,d}} \times \frac{[g(d, M)\lambda_k]^{N_d}}{N_d!},
 \end{aligned}$$

where  $\lambda_k = \sum_b \lambda_{b,k}$ . The marginal distribution of  $N_d$  is easily shown to be Poisson( $g(d, M)\lambda_k$ ). It follows that the conditional distribution is

$$(4) \quad \mathbf{R}_d | (Y = k, d, M, N_d) \sim \text{multinomial}(N_d; p_{1,k}, \dots, p_{B,k}),$$

where  $p_{b,k} = \lambda_{b,k}/\lambda_k, b = 1, \dots, B$ . Note that  $0 \leq p_{b,k} \leq 1$  and  $\sum_b p_{b,k} = 1$ . Hence, given  $N_d$ ,  $\mathbf{R}_d$  follows a multinomial distribution with the probability parameters  $p_{1,k}, \dots, p_{B,k}$  independent of  $d$ . In addition, by model (2),  $\mathbf{R}_{d(t)}, t = 1, \dots, T$ , at different distances are all independent. It follows that, if we were to base our inference conditioned on  $N_d$ , that is, the total radiation count at time  $d$  for all windows, we would not require any specific functional model for  $g(d, M)$  and  $N_d$ . The lower frame of Figure 1 corresponds to a real data example that validates this assumption. It can be seen that the ratio in counts between the two windows is approximately constant during the actual scan lasting around 23 seconds.

Let  $\mathbf{p}_k = (p_{1,k}, \dots, p_{B,k})'$  be named as the *energy spectrum* of the  $k$ th class in the rest of this paper. The energy spectrum is unique for a material class and invariant to  $g(d, M)$ . By the above derivation, we can simply focus on the energy spectrum  $\mathbf{p}_k$ . This is more pertinent and stable than the total radiation count  $N_d$ , which depends on the unknown  $g(d, M)$ . The disadvantage of using the conditioning likelihood is that it would not be possible to distinguish between two material classes that have an identical energy spectrum. We also remark that Ely et al. (2006) suggested that an energy windowing method should be used in conjunction with a gross counting threshold set at a relatively insensitive level.

The proposed conditional multinomial model has additional advantages as well. First, we can aggregate or disaggregate windows while keeping the new counts multinomial. Further, since our multinomial distribution depends on  $d$  only through  $N_d$ , we can pool the information from the counts obtained at many distances. We do not have to depend upon the radiation data at the maximum of  $N_d$  as the current approach does. Finally, conditioning on  $N_d$  allows us to implement a classification approach parallel to the naive Bayes classifier. We describe the development of the Bayesian classifier in the next two sections.

**3. Bayesian classifier.** For an introduction to the naive Bayes classification, we refer to Ye (2003) and Klosgen and Zytkow (2002). Here we construct a corresponding generative naive Bayesian classifier. We start with two distinct material

classes  $k$  and  $k'$ . By the Bayes theorem,

$$(5) \quad \frac{P(Y = k|\mathbf{Z})}{P(Y = k'|\mathbf{Z})} = \frac{P(Y = k)P(\mathbf{Z}|Y = k)}{P(Y = k')P(\mathbf{Z}|Y = k')},$$

where  $P(Y = k)$  and  $P(Y = k')$  are the prior probability. Apparently, a container is classified as class  $k$  if (5) is larger than 1. Generalizing this to  $K$  classes, we have the following classifier:

$$(6) \quad Y = \arg \max_{1 \leq k \leq K} [P(Y = k)P(\mathbf{Z}|Y = k)].$$

It is easily shown [Ferguson (1967)] that this rule is optimal in terms of Bayes risk as long as the cost of misclassification is the same across the categories.

The naive Bayesian classifier (6) has a convenient form for computation. Further conditioning on all  $N_{d(t)}$ ,  $t = 1, \dots, T$ , by (4), we have

$$(7) \quad P(\mathbf{Z}|Y = k, N_{d(1)}, \dots, N_{d(T)}) \propto \prod_b p_{b,c}^{\sum_d R_{b,d}}.$$

Equivalently, the classifier can be represented by the log likelihood

$$(8) \quad \begin{aligned} Y &= \arg \max_{1 \leq k \leq K} \left[ \sum_{b,d} R_{b,d} \log p_{b,k} + \log P(Y = k) \right] \\ &= \arg \max_{1 \leq k \leq K} [\mathbf{1}'\mathbf{Z}'(\log \mathbf{p}_k) + \log P(Y = k)]. \end{aligned}$$

This form of the naive Bayesian classifier is straightforward to compute, especially in the software packages optimized for matrix operations such as Matlab and R.

The naive Bayesian classifier (6) can be easily extended to accommodate differential losses to misclassification errors. Let  $W_{k',k}$  denote the cost of misclassifying a container to class  $k'$  when it actually belongs to class  $k$ . Let  $W_{k',k} = 0$  when  $k' = k$ . The expected loss of a classification is  $L(Y = k'|\mathbf{Z}) = \sum_{k=1}^K W_{k',k} P(Y = k|\mathbf{Z})$ . The optimal Bayesian decision rule is then  $Y_w = \arg \min_{k'} L(Y = k'|\mathbf{Z})$ . Note that (6) is a special instance using 0–1 loss of the decision rule  $Y_w$ .

The Bayesian classifier in this section assumes that the energy spectra  $\mathbf{p}_k$  is known for a variety of material classes. In the remainder of this section we discuss the Bayesian learning to reduce the uncertainty in estimating  $\mathbf{p}_k$  for both lab and field practices. Given  $Y = k$ , that is, the material class is known either by experimental set up or by an offline detailed inspection, we consider the conjugate prior for  $\mathbf{p}_k$ , that is, the Dirichlet( $\theta_{1,k}, \dots, \theta_{B,k}$ ) distribution. Then, training our classifier on the data obtained from past containers with known classes, we estimate  $\mathbf{p}_k$  by

$$(9) \quad \hat{p}_{b,k} = \left( \sum_{i,d} R_{b,d}^i + \theta_{b,k} \right) / \left( \sum_{i,b,d} R_{b,d}^i + \sum_b \theta_{b,k} \right),$$

where  $R_{b,d}^i$  is the radiation count for the  $i$ th container in the  $k$ th class. The summations over  $i$  are over the containers with class  $k$  contents in the training data.

For determining the parameters of the conjugate priors, one would typically use expert judgment. However, given the number of containers passing through U.S. ports, a prior is unlikely to have any significant effect on the ultimate decision except when the class is very rare. Typically, conjugate priors are somewhat restrictive in terms of the beliefs they can represent. Dalal and Hall (1983) and Diaconis and Ylvisaker (1985) show that an appropriate mixture of natural conjugate priors can approximate any arbitrary belief when the underlying distributions belong to an exponential family. Further, the corresponding posteriors converge almost surely to the true posterior. Given these results, it is possible to extend this development to mixtures of Dirichlet as priors for multinomial parameters. Using the results shown in those papers, it can be shown that the resulting estimates are the re-weighted mixtures of the estimates in (9).

**4. Asymptotic properties.** We have so far shown that the proposed procedure is an optimal Bayesian classifier. In this section we study the properties of our procedure for a fixed but arbitrary  $K$ , by the asymptotic means assuming the Poisson model (2) and the multinomial model (4), respectively.

We first consider the proposed classifier with  $K$  classes with energy spectra  $\mathbf{p}_k, k = 1, \dots, K$ , under the multinomial model (4) by conditioning on  $N = \sum_d N_d$ . For the development below, we consider the nontrivial case where all energy spectra are positive and distinct corresponding to each of the material class. Let  $\mathbf{p}_{k'}$  be the true energy spectrum. The optimal Bayes classifier is  $Y = k'$  if and only if (6) holds for  $Y = k'$ , namely,

$$k' = \arg \max_k P(Y = k)P(\mathbf{Z}|Y = k).$$

Taking log of ratio of the terms corresponding to  $k'$  and  $k$ , this is true if and only if

$$(10) \quad \log \frac{P(\mathbf{Z}|Y = k')P(Y = k')}{P(\mathbf{Z}|Y = k)P(Y = k)} \geq 0 \quad \text{for all } k.$$

Let  $L_b = \sum_d R_{b,d}$  and  $N = \sum_d N_d$ . Since  $(L_1, \dots, L_B)|N$  follows a multinomial distribution with parameters  $(N; \mathbf{p}_{k'})$ , by substituting the likelihood of  $P(\mathbf{Z}|Y)$  for  $Y = k$  and  $k'$ , we have (10) if and only if

$$(11) \quad \frac{1}{N} \left[ \sum_b L_b \log \frac{p_{b,k'}}{p_{b,k}} + \log \frac{P(Y = k')}{P(Y = k)} \right] \geq 0.$$

Since  $L_b$  follows binomial( $N, p_{b,k'}$ ), we have  $|L_b/N - p_{b,k'}| = o_p(1)$ . Further, the second term in (11) is  $O(N^{-1})$ . Thus, the left-hand side of (11) is

$$(12) \quad \sum_b \left[ p_{b,k'} \log \frac{p_{b,k'}}{p_{b,k}} + o_p(1) + O(N^{-1}) \right] = \eta(\mathbf{p}_{k'}, \mathbf{p}_k) + o_p(1)$$

as  $N \rightarrow \infty$ ,

where  $\eta(\mathbf{p}_{k'}, \mathbf{p}_k) = \sum_b p_{b,k'} \log \frac{p_{b,k'}}{p_{b,k}}$  is the Kullback–Leibler divergence between the two multinomial distributions with parameters  $(1; \mathbf{p}_{k'})$ , and  $(1; \mathbf{p}_k)$ . By the properties of the Kullback–Leibler divergence and the Gibbs’ inequality,  $\eta(\mathbf{p}_{k'}, \mathbf{p}_k) \geq \inf_{s, s \neq k'} \eta(\mathbf{p}_{k'}, \mathbf{p}_s) > 0$  for all  $k \neq k'$ . Thus,  $k'$  will be selected with probability approaching 1.

Now we generalize the above result, which says that our classifier is consistent for the multinomial case to the general Poisson case without conditioning on  $N$ . For the Poisson case, we have the total mean counts across  $d$  as  $\lambda_{k'} = \sum_{b,d} g(d, M) \lambda_{b,k'}$ . Suppressing the subscript  $k'$ , as  $\lambda \rightarrow \infty$ ,  $N/\lambda = 1 + o_p(1)$ , and thus, dividing the left-hand side of equation (10) by  $\lambda$  again gives equation (12). Thus, again,  $k'$  will be selected with probability approaching 1. Summarizing this, we have the following theorem.

**THEOREM 1.** *Under the multinomial model (4) and the Poisson model (2) and the assumption that all energy spectra  $\mathbf{p}_1, \dots, \mathbf{p}_K$  are distinguishable, as  $\lambda \rightarrow \infty$ , for a given true class  $k'$  in  $1, \dots, K$ ,  $P(Y = k' | \mathbf{Z}) \xrightarrow{P} 1$ .*

According to this result, irrespective of  $K$ , as long as all energy spectra are distinct, as the counts become large, the classifier proposed here will converge to the true underlying material. Further, it follows from the proof that for given counts, the probability of misclassification is higher for materials closer in the Kullback–Leibler divergence sense.

We now consider robustness of our procedure to changes in the true underlying energy distribution. By an argument that is an extension of the one used in proving the above theorem, the following theorem can be shown similarly.

**THEOREM 2.** *Under the multinomial model (4) and the Poisson model (2), and an arbitrary energy spectrum,  $\mathbf{p}^* = (p_1^*, \dots, p_B^*)$  not in  $\mathbf{p}_1, \dots, \mathbf{p}_K$ . Let  $k' = \arg \min_{1 \leq k \leq K} \eta(\mathbf{p}^*, \mathbf{p}_k)$ . Then as  $\lambda \rightarrow \infty$ ,  $P(Y = k' | \mathbf{Z}) \xrightarrow{P} 1$ .*

This result shows that even if the true distribution is not in the classification scheme, the ones closest to it will be selected. In this sense we have robustness with respect to variations in the underlying distribution.

**REMARK.** Robustness with respect to correlated data. In the development above, we assumed that  $R_{b,d}$  are all independent over  $d$ . One would expect by the underlying physics that radiation counts are independent in different time intervals. Given that our development parallels the naive Bayes models, it follows that the classifier (6) is robust to this violation. For further discussion of this we refer to Domingos and Pazzani (1997) and Zhang (2004) who show robustness of the models with violations to independence.



In summary, the results indicate that our procedure is robust with respect to variations in the underlying distribution and will scale up to large numbers of categories as long as the counts are large. The counts increase if either  $M$  increases, the speed of driving through the portal decreases or the number of  $d$ 's increase. Thus, from a policy perspective, for improving the detection probability, the most attractive option is to pool across  $d$ 's. It can also be shown by the Gibbs inequality that as the number of windows increases by further refinement, the corresponding Kullback–Leibler divergence between any two distributions also increases. Thus, for the next attractive option, one needs to carry out a cost–benefit analysis between reducing the speed and increasing the number of windows.

## 5. Numerical studies.

5.1. *Classification of all classes.* To explore and illustrate the sensitivity and specificity of our method, we consider a number of simulated examples and scenarios. The first example is based on energy spectra emitted by the following 7 classes of material: WGPu, HEU, fertilizer, tiles (refractory material), kitty litter, road salt and background (i.e., a container's radiation is undetectable from the background). The energy spectra were synthesized from a few sources, including Ely et al. (2004) and Ely et al. (2006), presentations from Pacific Northwest National Laboratory (PNNL) and consultation with PNNL scientists. For these data, the reported energy spectra only consisted of 3 windows. Table 1 lists the energy spectra of mean counts for 1 unit of the 6 pure material classes and background at the distance defined as  $d = 0$ . The man-made nuclear material classes were chosen based on their importance for detection in ports, while the NORM classes were selected based on their probability of misclassification indicated in Table 2 (courtesy of PNNL). Radiation from the NORM classes is primarily from potassium-40, which naturally exists in many common materials. For reference, false positive probabilities for some typical NORM materials are shown in Table 2 (compiled

TABLE 1  
*The energy spectra for the 6 pure material classes and background. Numbers in parentheses are  $\lambda_{b,k}$*

Class	Window 1	Window 2	Window 3
HEU	0.954 ( $1.77 \times 10^4$ )	0.033 (616)	0.013 (247)
Fertilizer	0.635 ( $2.72 \times 10^3$ )	0.243 ( $1.0 \times 10^3$ )	0.122 (519)
Tile	0.658 ( $2.22 \times 10^3$ )	0.242 (818)	0.100 (338)
WGPu	0.934 ( $6.09 \times 10^4$ )	0.061 ( $3.9 \times 10^3$ )	0.005 (285)
Kitty litter	0.631 ( $1.7 \times 10^3$ )	0.292 (790)	0.077 (208)
Road salt	0.662 ( $2.1 \times 10^3$ )	0.273 (873)	0.065 (208)
Background	0.651 ( $1.4 \times 10^3$ )	0.249 (519)	0.100 (207)

TABLE 2

*Some frequently misclassified NORM classes by the currently deployed methodology. Numbers are proportions of false positive for detecting radiation risk*

Source class	Port A	Port B	Port C
Kitty litter	0.34	0.25	–
Abrasive pads	0.14	0.05	–
Mica	0.05	–	–
Fertilizer	0.05	0.13	–
Ceramics/tile	0.04	0.09	0.28
Granite	0.04	–	0.10
Salt	–	0.05	–
Trucks/cars	0.02	–	–
Aluminum	–	0.15	–
Other metal	–	0.03	–

from personal communications with PNNL), per the currently deployed method and publicly available data. The units of quantity are different for different classes. Ely et al. (2004) and Ely et al. (2006) considered 1 unit WGPu as 99.4 g in a powdered oxide form and doubly contained in schedule-80 stainless steel closed pipes that provide shielding. Even with shielding, 1 unit WGPu is still highly radioactive. 1 unit HEU was considered as 123 g of 93.1% enriched uranium consisting of a number of stacked foils, which is a moderately strong radiation source. For all NORM material classes, 1 unit is 5 kg. We also consider another man-made class as a mixture of 0.5 unit HEU and 0.5 unit of WGPu.

To numerically simulate the radiation data, we set up  $g(d, M) = (1 - d)M$  and 20 distances (0.9, 0.8, ..., 0.1, 0, 0, 0.1, ..., 0.9), corresponding to the portal passing-through time for a container. As discussed previously, the specific form of  $g(d, M)$  does not affect the Bayesian classifier, but is only needed for generating data. This simulation scenario is set up to have the total counts  $\sum_d N_d$  comparable to the actual scanning process shown in Figure 1. In the first simulation study, we generated 10,000 samples of Poisson variables at each  $d$  for a variety of material classes. We assign a prior probability  $10^{-9}$  to each man-made source, and use equal prior probability for each NORM class. Table 3 reports the misclassification probabilities. The Bayesian classifier has excellent performance in this scenario. It was able to classify all materials correctly except for minor confusion between tiles and background, both not dangerous. In particular, there is no misclassification between man-made source and NORM in 10,000 simulations.

**REMARK.** At this scale of total counts, the classifier is relatively insensitive to the choice of prior  $P(Y = k)$ . From (8), it can be seen that as long as  $\log(P(Y = k)) = o_p(\mathbf{1}'\mathbf{Z})$ , the prior should have no practical impact on the classifier. Recall that the actual counts are large (see Figure 1). Hence, the prior probability for man-made source is unlikely to influence the classification remarkably. Since the total

TABLE 3

Summary of classification simulations with 8 classes. Classes A to H are WGPu (A), HEU (B), mixture of 0.5 unit. WGPu and 0.5 unit HEU (C), fertilizer (D), tile (E), kitty litter (F), salt (G) and background (H)

True class	Classified							
	A	B	C	D	E	F	G	H
A	1	0	0	0	0	0	0	0
B	0	1	0	0	0	0	0	0
C	0	0	1	0	0	0	0	0
D	0	0	0	1	0	0	0	0
E	0	0	0	0	0.937	0	0	0.063
F	0	0	0	0	0	1	0	0
G	0	0	0	0	0	0	1	0
H	0	0	0	0	0.111	0	0	0.889

counts in simulations are also large (comparable to Figure 1), there is not a single change in misclassifying a man-made source to NORM, or vice versa, if we use the equal prior probability on all classes, or change the prior probability of each man-made source to  $10^{-9}$ .

We now study a more complex situation by considering a more devious terrorist strategy of mixing materials. The man-made source possessed by terrorists, such as WGPu or HEU, may be mixed with a NORM material class. Moreover, the total count may be made small enough to pass the current inline inspection. Hence, to challenge the classifier, the main sensitive material classes should allow mixtures of man-made and NORM classes. For hard to detect situations, the mixture should have a small quantity of a man-made source and a relatively large quantity of NORM. In the next numerical study, we consider this possibility by using a list of mixtures of the known classes except for background. Each mixture class mixes WGPu or HEU with one of the 4 NORM classes. Assuming that the mixture is noninterfering, the energy spectrum for the mixture of two classes  $k$  and  $k'$  with quantities  $M$  and  $M'$  will be given by

$$(13) \quad \frac{[(1-d)M\lambda_{b,k} + (1-d)M'\lambda_{b,k'}]}{\sum_b [(1-d)M\lambda_{b,k} + (1-d)M'\lambda_{b,k'}]}, \quad b = 1, \dots, B.$$

We considered 3 small quantities for each man-made source class to simulate the different diluting effects. The quantity of HEU was 0.025, 0.05 or 0.1 unit, and the quantity of WGPu was 0.005, 0.01 or 0.025 unit. The quantity of HEU is slightly larger than WGPu due to the relatively weaker radioactivity by the definition of 1 unit HEU. All of the classes being inspected except for background have the same mean count in the first window. Since the first window has much larger counts than the other two windows, a real container of all these classes will have

approximately the same total counts. We set the mean count at distance  $d = 0$  in the first window,  $M\lambda_{1,k} + M'\lambda_{1,k'}$  at 3000 for all mixture classes. The quantity of all NORM classes is solved from the preceding restriction. For example, the mixture class “0.025HEU + Fertilizer” has 0.025 unit HEU and 0.941 unit fertilizer. The mean value 3000 was set to be close to 1 unit of NORM and far less than 1 unit of a man-made source, representing a scenario that could be encountered at port inspection. It is likely that the currently deployed method will not detect most of the containers with small quantities of HEU or WGPu, since it is based on maximal gross counts. We also considered the 4 pure NORM classes and the background. Except for background, the quantities of the 4 NORM classes were set according to  $M\lambda_{1,k} = 3000$ . For instance, the pure kitty litter class under this constraint has 1.759 units. This gave a total of 29 material classes to be classified. We call the mixture classes with man-made source as *dangerous* classes, and the NORM classes and background as *nondangerous* classes. Since the material classes have energy spectra consisting of 3 windows, we can plot the corresponding proportion of spectra in two energy windows, which is shown in Figure 2. As can be seen, some dangerous and nondangerous classes are intermingled.

The Bayesian classifier again has very good performance in this scenario. For all dangerous classes, the misclassification probability is below 0.005 (including misclassified as other dangerous classes). Most of the misclassification probabilities for NORM classes are below 0.01, except for the misclassifications between tile and background (0.06 for misclassifying tile as background, and 0.11 for misclassifying background as tile). This indicates that the Bayesian classifier scales well and is hard to defeat by the simple strategy of mixing a man-made nuclear material with a NORM.

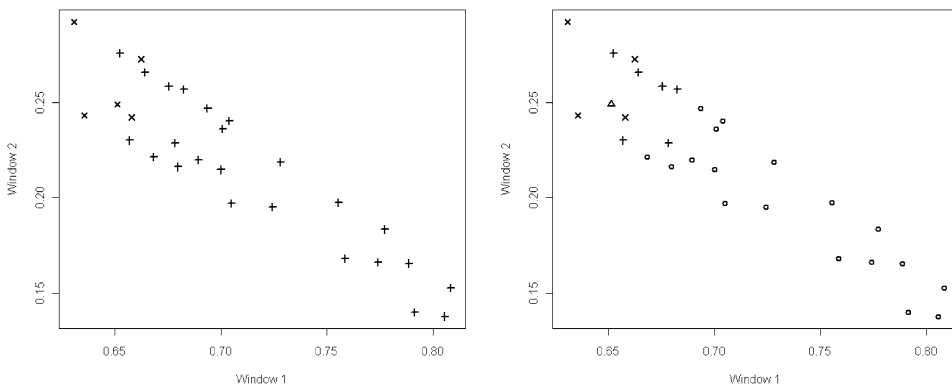


FIG. 2. Illustrations of classes. The left frame has all 29 classes as benchmark and the right frame has 10 automatic selected benchmarks. Circle: dangerous nonbenchmark; cross: dangerous benchmark;  $\times$ : nondangerous benchmark; triangle: nondangerous nonbenchmark.

5.2. *Classification into dangerous versus nondangerous classes.* In the previous section we examined the problem of exact classification of all materials, and, consequently, we used all material classes to build the classifier. Here we consider a more limited objective for preliminary screening, namely, classify a given material as dangerous or nondangerous from a given large list of  $K$  dangerous (material involving man-made nuclear sources including mixtures) and nondangerous materials. After classifying in these categories, one can use a scheme akin to the previous section to identify the specific dangerous material at the next stage.

Given this limited objective, and that there may not be any natural differentiation (e.g., hyperplane in some transformed space) in the spectra profile of dangerous and nondangerous materials, this problem cannot be solved by the standard binary classification methods. Instead, we consider the following scheme, whereby we build the classifier based on a subset of materials (called *benchmark classes*) from the list. A material is classified as dangerous if the corresponding selected benchmark material is dangerous; otherwise it is nondangerous.

For this setting, the simplest scheme would be to use all materials as benchmark classes. The question we address is the following: can one be more parsimonious in the number of benchmark materials to build the classifier? Having a smaller number of benchmark classes of materials should help in scaling up the solution. Below we first investigate this question in the context of 29 materials considered in the last subsection and compare this “all classes” solution with an algorithmically derived solution.

The algorithm to select benchmark classes is iterative and does not require specific structure of the materials. It is motivated by the support vector machine method and forward selection method [Hastie, Tibshirani and Friedman (2009)]. However, unlike the support vector machine method, which finds the separating hyperplane with the biggest margin, we identify high leverage points that are difficult to distinguish and use them as benchmark classes and we iterate on the scheme by forward selection. Given that the total counts are large in our applications, for identifying a high leverage point, we revert to Theorem 2, which states that if a class is not in the classifier, the class nearest in the Kullback–Leibler sense will be selected by the classifier. For describing the algorithm, the following notation is in order. Suppose that of the  $K$  major distinct classes,  $K_1$  classes are dangerous, and  $K_2$  classes are nondangerous, all with distinct energy spectra. Let  $D$  and  $ND$  be the corresponding sets of material. At the  $i$ th iteration, the algorithm produces a list of dangerous and nondangerous material to be used as the benchmark class for the next stage, and let us denote those subclasses as  $D_i$  and  $ND_i$ . Finally, let  $\eta(\mathbf{p}, A) = \inf\{\eta(\mathbf{p}, \mathbf{p}_k), k \in A\}$ , where  $\eta(\mathbf{p}, \mathbf{p}_k)$  is the Kullback–Leibler divergence defined in Section 4. The algorithm for selecting benchmark classes is as follows.

ALGORITHM.

(a) For  $i = 1$ , initiate by taking  $D_1$  and  $ND_1$  to be any pair of dangerous and nondangerous material which are nearest in  $\eta^*$ , the symmetrized version of  $\eta$  [i.e.,  $\eta^*(\mathbf{p}, \mathbf{q}) = \eta(\mathbf{p}, \mathbf{q}) + \eta(\mathbf{q}, \mathbf{p})$ ].

(b) At the stage  $i + 1$ , let  $AD_{i+1} = \{k : k \in D - D_i, \eta(\mathbf{p}_k, D_i) - \eta(\mathbf{p}_k, ND_i) > 0\}$  and  $AND_{i+1} = \{k : k \in ND - ND_i, \eta(\mathbf{p}_k, ND_i) - \eta(\mathbf{p}_k, D_i) > 0\}$ . Note that if the total counts are large,  $AD_i$  will be misclassified with high probability as nondangerous and vice versa.

(c) If  $AD_{i+1}$  and  $AND_{i+1}$  are empty, then stop. Otherwise  $D_{i+1} = D_i \cup k^*$ , where

$$k^* = \arg \min_{k \in AD_{i+1}} \eta(\mathbf{p}_k, ND_i).$$

Similarly construct  $ND_{i+1}$ .

(d) Repeat this process till  $AD_{i+1}$  and  $AND_{i+1}$  are empty. Note that when we stop, we have asymptotically probability 1 of correct classification of materials in dangerous and nondangerous classes.

In our previous example with 29 classes, the above algorithm leads to only 10 benchmark classes. Table 4 gives the corresponding probabilities of misclassification. All solutions have exceptional performance and are indistinguishable. Based on this comparison, if the binary classification is the main objective, it would be always preferable to use the algorithmic approach, since it reduces the complexity without penalizing performance. Further, it does not require any specific structure of the materials.

Next, we examine the performance of the algorithm in a large study with 100 classes, consisting of 75 dangerous and 25 nondangerous. The dangerous classes

TABLE 4

*Summary of simulations with 29 classes: numbers are the probability of detecting dangerous radioactive materials. The two columns under each class correspond to all 29 classes as benchmark and the automatic selected benchmark. The selected benchmark classes are marked with a star*

0.025HEU + Fertilizer	1	1	0.005WGPu + Fertilizer*	1	1
0.05HEU + Fertilizer	1	1	0.01WGPu + Fertilizer	1	1
0.1HEU + Fertilizer	1	1	0.025WGPu + Fertilizer	1	1
0.025HEU + Tile	1	1	0.005WGPu + Tile*	1	1
0.05HEU + Tile	1	1	0.01WGPu + Tile	1	1
0.1HEU + Tile	1	1	0.025WGPu + Tile	1	1
0.025HEU + Kitty litter*	0.997	0.997	0.005WGPu + Kitty litter*	0.999	1
0.05HEU + Kitty litter	1	1	0.01WGPu + Kitty litter*	0.999	1
0.1HEU + Kitty litter	1	1	0.025WGPu + Kitty litter	1	1
0.025HEU + Salt	1	1	0.005WGPu + Salt*	1	1
0.05HEU + Salt	1	1	0.01WGPu + Salt	1	1
0.1HEU + Salt	1	1	0.025WGPu + Salt	1	1
Fertilizer*	0	0	Tile*	0	0
Kitty litter*	0	0	Salt*	0.011	0.012
Background	0	0			

were mixtures of a man-made source with 4 NORM classes. The quantity of man-made source was either 0.025 unit HEU or 0.005 WGPu, and the quantities of 4 NORM classes were generated from a Dirichlet distribution with parameters (0.25, 0.25, 0.25, 0.25). The nondangerous classes were mixtures of 4 NORM classes, and the quantities were generated independently from  $U(0, 0.25)$ . This scenario is more stringent than the previous scenarios, since this scenario uses the smallest quantities of man-made sources used in the previous scenarios. We generated 50 sets of classes. The mean number of benchmark classes chosen by the algorithm is 6.9 and the standard deviation (sd) is 5.7. The median number of benchmark classes is 5 and the median absolute deviation (mad) is 6. For each of the 50 sets of generated classes, we ran 1000 simulations to evaluate the performance. The mean probability of misclassifying a dangerous class as nondangerous is 0.001 (median = 0.000, sd = 0.009, mad = 0.000), and the mean probability of misclassifying a nondangerous class as dangerous is 0.008 (median = 0.000, sd = 0.037, mad = 0.000).

In summary, the numerical examples in this section show that the parsimonious benchmark classes chosen by the proposed algorithm retain the capability of detecting illicit nuclear material and are more efficient in computation.

**6. Discussion.** We have proposed a Bayesian approach for modeling the energy distribution as well as the total energy emitted by an unknown material class. We have also proposed a Bayesian decision rule for classifying a new container into one of the known classes. Our approach uses all available data compared to the currently deployed method, which only uses the maximal counts. We have examined its robustness properties by simulations and asymptotic arguments and have shown that the proposed approach is scalable. For binary classification between dangerous and nondangerous materials, we have proposed a scalable algorithm for selecting a small number of benchmark classes motivated by the support vector machine and forward selection methods. The results in this paper are encouraging compared to the false positives reported by the currently deployed method in Table 2.

Since our approach is based on classification, two questions naturally emerge for our and other classification approaches, namely, (1) to what extent is the procedure robust with respect to variation in the underlying distribution? and (2) to what extent can one entertain the possibility of none of the above classes? Theorem 2 and ensuing discussion show that our approach is robust in the sense that even if the true distribution is not in the classifier, the benchmark class closest to it will be selected. While our and all other classification approaches do not allow a direct answer to the second question, it should be feasible to perform a Chi-squared goodness of fit test for the selected class. If such a test rejects the hypothesis, then one possibility is to screen such a container. Clearly, the efficacy of such a simultaneous procedure needs to be further investigated. Also, since our approach does not depend upon the number of windows and the time to pass-through the portal, it

is likely to be easily extendable to newer portals, more windows, material classes and changes in design.

**Acknowledgments.** The authors wish to thank James Ely, Dennis Weier, Rick Bates and the rest of the PNNL team for sharing information and helpful discussions, and Fred Roberts and Tami Carpenter of DIMACS at Rutgers University for getting the authors involved in this problem of national security. The authors also thank Colin Mallows of Avaya Labs for helpful comments, and the referee and Associate Editor for helpful comments.

## REFERENCES

- DALAL, S. and HALL, W. J. (1983). Approximating priors by mixtures of natural conjugate priors. *J. Roy. Statist. Soc. Ser. B* **45** 278–286. [MR0721753](#)
- DIACONIS, P. and YLVIKAKER, D. (1985). Quantifying prior opinion. In *Bayesian Statistics 2* (J. Bernardo, M. DeGroot, D. Lindley and A. Smith, eds.) 133–156. North-Holland, Amsterdam. [MR0862488](#)
- DOMINGOS, P. and PAZZANI, M. (1997). On the optimality of the simple Bayesian classifier under zero–one loss. *Mach. Learn.* **29** 103–130.
- ELY, J., KOUZES, R., GEELHOOD, B., SCHWEPPE, J. and WARNER, R. (2004). Discrimination of naturally occurring radioactive material in plastic scintillator material. *IEEE Transactions on Nuclear Science* **51** 1672–1676.
- ELY, J., KOUZES, R., SCHWEPPE, J., SICILIANO, E., STRACHAN, D. and WEIER, D. (2006). The use of energy windowing to discriminate SNM from NORM in radiation portal monitors. *Nuclear Instrument and Methods in Physics Research Section A* **560** 373–387.
- FERGUSON, T. S. (1967). *Mathematical Statistics: A Decision Theoretic Approach*. Academic Press, New York. [MR0215390](#)
- HASTIE, T., TIBSHIRANI, R. and FRIEDMAN, J. (2009). *The Elements of Statistical Learning: Data Mining, Inference, and Prediction*, 2nd ed. Springer, New York.
- KARLIN, S. and TAYLOR, H. (1998). *An Introduction to Stochastic Modeling*. Academic Press, San Diego, CA. [MR1627763](#)
- KLOSGEN, W. and ZYTKOW, J. (2002). *Handbook of Data Mining and Knowledge Discovery*. Oxford Univ. Press, New York.
- MARTONOSI, S., ORITZ, D. and WILLIS, H. (2006). Evaluating the viability of 100 percent container inspection at America’s ports. In *The Economic Impact of Terrorist Attacks* (H. W. Richardson, P. Gordon and J. Moore II, eds.) 218–241. Edward Elgar Publishing, Northampton, MA.
- WEIN, L., WILKINS, A., MAVEN, M. and FLYNN, S. (2006). Preventing the importation of illicit nuclear materials in shipping containers. *Risk Analysis* **26** 1377–1393.
- YE, N. (2003). *The Handbook of Data Mining*. LRA, Mawah, NY.
- ZHANG, H. (2004). The optimality of naive Bayes. In *Proceedings of the Seventeenth International Florida Artificial Intelligence Research Society Conference* (V. Barr and Z. Markov, eds.) 133–156. AAAI Press, Menlo Park, CA.

RAND CORPORATION  
1776 MAIN ST.  
SANTA MONICA, CALIFORNIA 90401  
USA  
E-MAIL: [sdalal@rand.org](mailto:sdalal@rand.org)